Available online at www.sciencedirect.com

ScienceDirect

ARTICLE

Effect of Nb Solute Concentration on Crystallite Size Refinement and Strength Enhancement in Mechanically Alloyed Cu-Nb Alloys

Lei Ruoshan[1], Chen Guangrun[1], Wang Mingpu[2]

[1] China Jiliang University, Hangzhou 310018, China; [2] Central South University, Changsha 410083, China

Abstract: Cu-Nb alloys with a Nb concentration range of 0 wt%~30 wt% were prepared by mechanical alloying (MA) at room temperature. The effects of Nb content on the crystalline refinement process and mechanical properties of the immiscible Cu-Nb system were investigated by X-ray diffraction (XRD), optical microscopy (OM), scanning electron microscopy (SEM) with energy-dispersive X-ray detection (EDX), transmission electron microscopy (TEM) and microhardness measurement. Results show that the completed dissolution of Nb in Cu can be achieved in the samples with Nb content less than ~11 wt% after 100 h milling, although the equilibrium solubility level is nearly zero. The grain size refinement capability of MA-ed Cu-Nb powder is enhanced with increasing Nb content up to 30 wt%. This is because the susceptibility to recovery process becomes reduced, when the amount of Nb solutes segregated into the dislocation of Cu phase is increased. Cu-30wt%Nb powder milled for 100 h, the average Cu grain size is only ~6 nm. The microhardness of the samples shows an enhancement with increasing Nb concentration. The main strengthening mechanisms of the MA-ed Cu-Nb alloys are linked to the grain size reduction and the dissolution of Nb into Cu matrix.

Key words: copper based alloy; nanocrystalline; mechanical alloying; supersaturated solid solution; microhardness

Copper based alloys have been an extensive subject of interest due to their versatility in the field of engineering applications, such as spot welding, electrical contacts and high performance switches[1, 2]. In order to satisfy modern day demand, many efforts have been made to improve the mechanical properties and thermal stability without sacrificing the electrical conductivity of Cu based alloys. It has been proved that the addition of insoluble elements (such as Mo, Nb, Fe, W and Cr) is an effective way[3-6]. Once the insoluble element is dissolved into the Cu matrix, it will precipitate to form fine insoluble particles as the strengthening phase and keep the matrix clean to retain a good electrical conductivity by a heat treatment at high temperatures. Among these alloys, nanocrystalline Cu-Nb alloys exhibit a good combination of mechanical strength, electrical property, thermal stability and radiation tolerance[6-13].

Due to the negligible solid solution solubility between Cu and Nb (~0.1 at%Nb), the formation of supersaturated Cu-Nb solid solutions is only possible using non-equilibrium techniques such as mechanical alloying (MA), rapid solidification processing and plasma processing[9-11, 14]. It has been proved that MA is an effective method to produce supersaturated Cu-Nb nanocrystalline solid solutions [9-11]. Ref.[11] has reported that up to 10 at%Nb can be forced into the Cu matrix by cryogenic ball milling. The extended solid solution of Nb in Cu by MA has been attributed to the dislocation solute-pumping mechanism and also the nanocrystalline microstructure[11, 15, 16]. Though some of the prior literatures have investigated the micro-structural evolution as a function of the milling conditions (milling time and temperature), none of them explicitly explain how the solute behavior affects the MA process and defines the end MA products. In fact, even though the

nanocrystalline structures have been observed in most MA-ed materials, the alloying effect on the formation of nanocrystalline grains still lacks systematic investigations.

In this paper, a series of Cu-xNb (x=0wt%~30wt%) alloys were prepared by MA. The influences of Nb content on the phase and microstructural evolutions, as well as the mechanical property of these alloys have been explored using a combination of X-ray diffraction (XRD), optical microscopy (OM), scanning electron microscopy (SEM), transmission electron microscopy (TEM) and Vickers hardness measurements. The relationship between the Nb solute and the formation of nanostructure was discussed. It is found that the inherent microstructure, the crystallite refinement process as well as the mechanical strength of the alloys are closely related to the Nb solute.

1 Experiment

Cu-Nb alloys were prepared using MA at room temperature. Nb was added into Cu in concentrations (wt%) of 0, 5, 10, 15, 20 and 30. The Cu powder had a purity of ~99.6%, with an average particle size of ~50 μm, while the corresponding values for Nb powder were ~99% and ~10 μm. The MA process was performed in a QM-1SP4 planetary ball milling with stainless steel vials and balls at a rotor speed of 300 r/min. The ball to powder mass ratio was kept to be 15:1. All of the powder particles were milled at various intervals up to 100 h, and a small amount of powders was extracted at each time interval for investigation. All of the milling process and the sample handling were carried out under an argon atmosphere. To avoid excessive heating, all of the milling operations were stopped for 20 min after each 15 min milling.

XRD analysis of the as-milled powders was performed using a DMAX2000 X-ray diffractometer and Cu Kα radiation (λ=0.154 nm) at a scan rate of 1°/min. Williamson-Hall method was used for the grain size and internal strain determinations after subtracting instrumental broadening[16]. After polishing and etching in a solution (5 g FeCl$_3$ + 25 mL HCl + 100 mL H$_2$O), the milled powders were observed on the LEICA EC3 optical microscopy. SEM with energy-dispersive X-ray detection (EDX) analyses of the powders were carried out on a Sirion 200 scanning electron microscope using 20 kV beam energy. A JEOL JEM-2100 with a point resolution of 0.19 nm was used to perform TEM and high-resolution TEM (HRTEM) observations, which were operated at 200 kV. The microhardness of the samples was measured on a HVA-10A Vickers microhardness tester using 2 kg load with a dwell time of 30 s. The average microhardness values were obtained after at least 10 measurements.

2 Results

2.1 XRD analysis

The XRD technique was used to study the evolutions of Cu-Nb alloys during milling. For simplicity, only the representative XRD patterns from pure Cu and Cu-30wt%Nb alloy as a function of MA time are plotted in Fig. 1a and 1b, respectively. The primary Cu and Nb peaks show peak intensity fading and peak broadening with the extended milling time. This can be attributed to the grain refinement and lattice distortion induced by the severe plastic deformation during MA[17,18]. On the other hand, the positions of Cu peaks do not change for pure Cu with increasing milling time (Fig. 1a). Whereas, there is a notable shift to lower angles for the Cu peaks in Cu-30wt%Nb alloy, suggesting the Cu lattice expansion (Fig.1b). The occurrence of Cu lattice expansion is due to the diffusion of the larger Nb solute atoms into the Cu matrix. The same phenomena are also observed for other samples containing 5 wt%~20 wt% of Nb during milling.

Fig. 1c shows the XRD patterns of 100 h milled Cu-Nb powders with different Nb concentrations. It can be seen that no diffractions of Nb element can be found in the samples with Nb content lower than 15 wt%, indicating the formation of supersaturated Cu-Nb solid solution. However, the existence of $(110)_{Nb}$ peak reveals that there are still a few undissolved Nb particles in these samples with Nb content in the range of 15 wt%~30 wt%. On the other hand, the Cu diffraction peaks become broader and their intensities get lower with the increasing Nb concentration, indicating the possible microstructural change of the samples.

Fig. 2 shows the calculated Cu lattice parameters for 100 h milled Cu-Nb samples as a function of Nb concentration. An increase of the Cu lattice parameter can be observed from ~0.3618 to ~0.3642 nm with increasing Nb content from 0 wt% to 10 wt%. After this point, the Cu lattice parameter increases quite slightly with higher Nb concentration, suggesting a further dissolution of Nb in Cu is limited. The dissolved Nb content in the milled Cu-Nb solid solution after 100 h milling can be calculated based on the Vegard's method:

$$(1-x)a_1 + xa_2 = a \tag{1}$$

where a, a_1 and a_2 represent the lattice parameters of the solid solution, pure solvent element ($a_{1\text{-Cu}}$ = 0.3615 nm) and solute element ($a_{2\text{-Nb}}$=0.4045 nm), respectively, and x is the solid solubility[5,19]. Accordingly, the quantity of dissolved Nb in Cu for the 100 h milled Cu-10wt%Nb and Cu-30wt%Nb samples can be determined to be ~9.2 wt% and ~11.2 wt%, respectively. Thus, a supersaturated state of the Cu matrix may be reached with ~11 wt%Nb under the present milling condition.

The average crystalline grain size and internal strain of Cu matrix can be determined from the broadening of the Cu peaks. Fig. 3a illustrates that the changing trend of the average Cu grain size for these samples is similar during
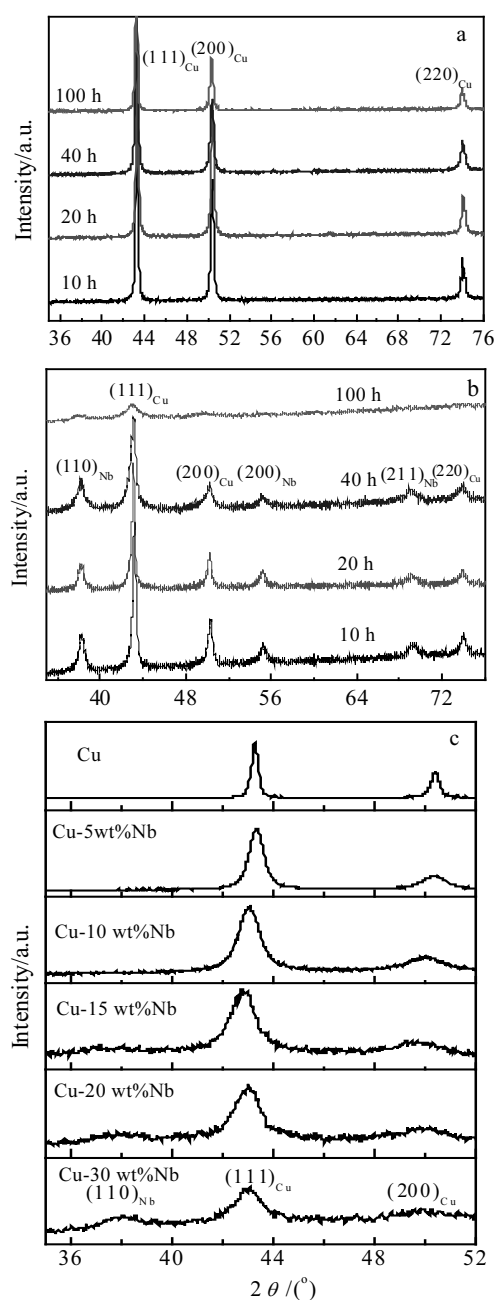
Fig.1   Evolutions of XRD patterns of Cu (a) and Cu-30wt%Nb powders (b) as a function of MA time; (c) XRD patterns of 100 h milled Cu-Nb alloys with different Nb contents
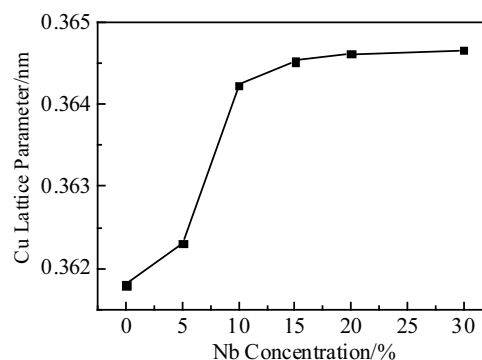

Fig.2   Cu lattice parameter for Cu-Nb samples milled for 100 h versus the Nb concentration
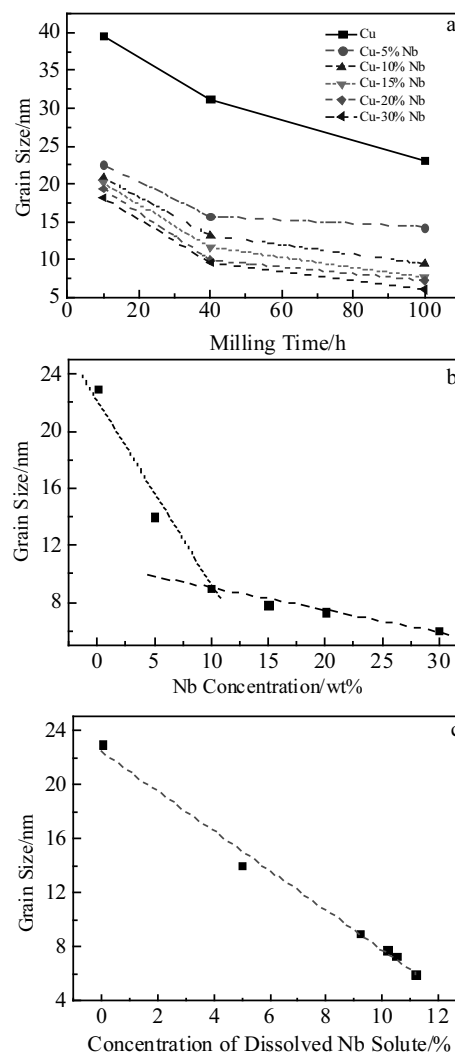

Fig.3   Mean grain sizes of Cu matrix as a function of milling time for the Cu-Nb powders with different concentrations (a), mean Cu grain size of 100 h milled samples as a function of Nb concentration (b); mean Cu grain size of the 100 h milled samples as a function of Nb solute content into solution (c)

milling. The mean Cu grain sizes are found to decrease fast within the first 40 h milling, and decrease slowly by further milling. Fig.3b plots the mean Cu grain size of the 100 h milled Cu-Nb powders as a function of the Nb concentration. The grain size is estimated to be ~23 nm for 100 h milled pure Cu, whereas it decreases to the smallest value of ~6 nm for Cu-30wt%Nb sample. More importantly, two different types of linear trends are found for the data points. It is obvious that the decreasing rate of grain size with Nb concentration is rapid for the samples containing 0wt%

~10wt% Nb, and then the reduction of Cu grain size slows down considerably with further increasing Nb concentration. This strongly suggests that grain refinement process of the MA-ed Cu-Nb alloys is not only related to the milling energy but also to the Nb solute.

To explore the influence of dissolved Nb solute atoms on the Cu grain refinement, the relationship between the final Cu grain size and the concentration of Nb solute dissolved in solid solution (estimated via the Vegard's method) is given in Fig.3c. It can be seen that there is a linear correlation between the dissolved Nb content and Cu grain size of the samples. If this trend is extrapolated to a grain size of zero, the quantity of dissolved Nb solute content is estimated to be ~22 wt%Nb. This value is in agreement with the thermodynamic analysis in Ref.[20, 21], where the crystal-to-amorphous transition is reported to occur due to the smaller molar enthalpy of amorphous phase than that of Cu-Nb solid solution with the composition in the range of 19 wt%~91 wt%Nb. However, the amorphous state is unachieved in Cu-20wt%Nb and Cu-30wt%Nb samples milled for 100 h in the present study, since the maximum solid solubility of Nb into Cu is about 11 wt%Nb. For the samples with 15 wt%~30 wt%Nb, the undissolved Nb particles which can act as grinding aids may further promote the slight reduction of Cu grain size.

As shown in Fig.4a, the Cu internal strains of all the samples are enhanced significantly during the first 40 h of milling. As the milling time is further increased from 40 to 100 h, the increasing rates of internal strains decrease. Fig. 4b displays the variation of the Cu internal strains in the 100 h milled samples as a function of Nb content. It can be seen that the internal strain exhibits a rapid enhancement with Nb concentration from 0 wt% to 10 wt%, and asymptotically reaches an almost saturated value of ~1.36%. As the powder particles experience the repeated fracturing, cold welding and severe plastic deformation during MA, the internal strain enhancement primarily results from the increase in the dislocation density.

2.2 OM observation

To illustrate the morphology evolution of the powder mixtures during milling, the OM images of Cu-15wt%Nb sample milled for different time have been given in Fig.5. After 1 h milling, the soft Cu particles begin to weld together to form the original lamellar structure, and the brittle Nb particles (as marked by the black arrows) get trapped in the Cu particles (Fig. 5a). With further milling, the layered structure continues to refine and becomes convoluted due to the repeated deformation, random welding and fracture (Fig. 5b and Fig. 5c). Meanwhile, an obvious increase in the powder size can be observed at this stage. By further milling, the brittleness of the powders increases and the fracturing tendency becomes dominant due to work hardening, leading to the reduction of the powder sizes (Fig. 5d).
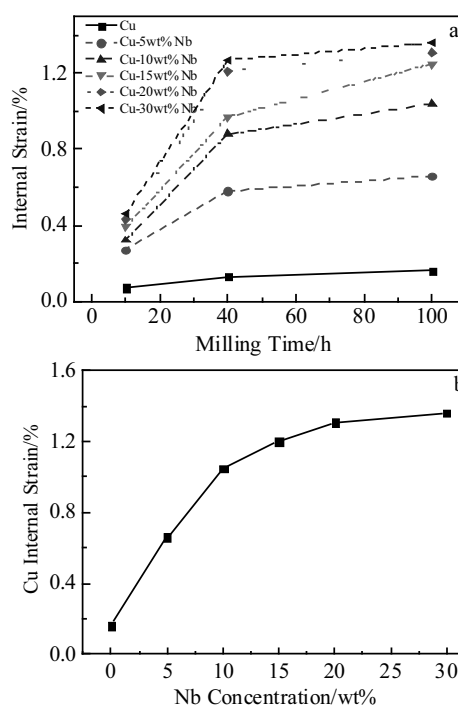

Fig.4 Evolutions of the mean Cu internal strains as a function of milling time for Cu-Nb powders with different Nb concentrations (a); mean Cu internal strain of Cu-Nb samples milled for 100 h as a function of Nb concentration (b)

2.3 SEM observation

As shown in Fig.6a~6c, the bright Nb particles are still visible in the Cu-10wt%Nb, Cu-15wt%Nb and Cu-30wt% Nb powders milled for 40 h. In the case of Cu-30wt%Nb, there are a number of large undissolved Nb particles distributed in the Cu matrix (Fig.6c). EDX analysis of the Nb particle marked by the plus sign in Fig.6c reveals a Cu content of ~7.3wt%, while the Cu region marked by the box sign in Fig.6c shows a Nb content of ~24.1wt%, indicating the interdiffusion between Nb and Cu during milling. Increasing milling time to 100 h results in the formation of a homogeneous microstructure and no Nb particles remain in Cu-10wt%Nb powders (Fig.6d). For the samples with Nb concentration higher than 10wt%, though the complete dissolution of Nb into the Cu matrix has not been achieved, the volume fraction and the size of remained Nb particles are much smaller compared with those milled for 40 h (Fig. 6e~6g).

2.4 TEM observation

Fig.7a shows the TEM bright-field (BF) image of Cu powders milled for 100 h, where a nanocrystalline microstructure with Cu grain size in the region of 20~70 nm is observed. It should be pointed out that the Cu grain size determined from TEM images is larger than that estimated by XRD technique, which is common in the severe plastic
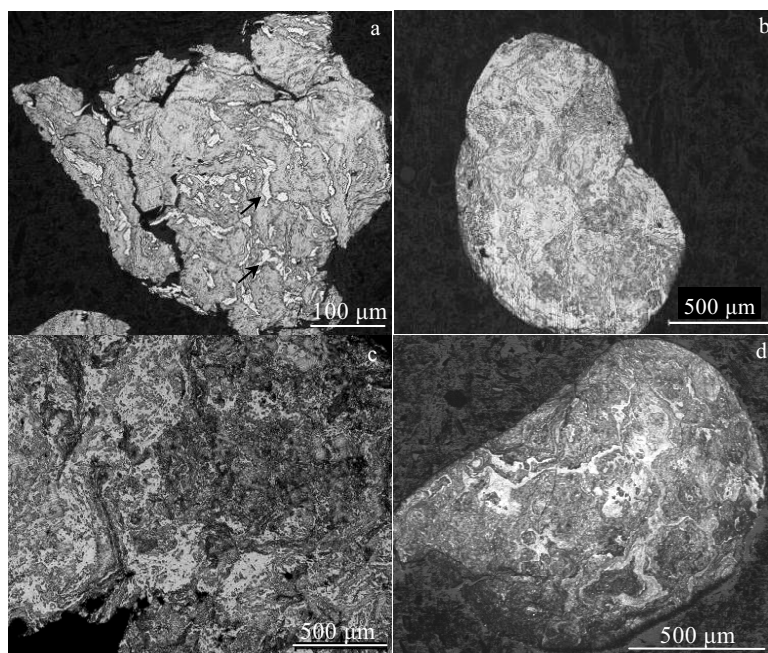
Fig.5   OM images of Cu-15wt%Nb powders after milling for 1 h (a), 10 h (b), 40 h (c) and 100 h (d)
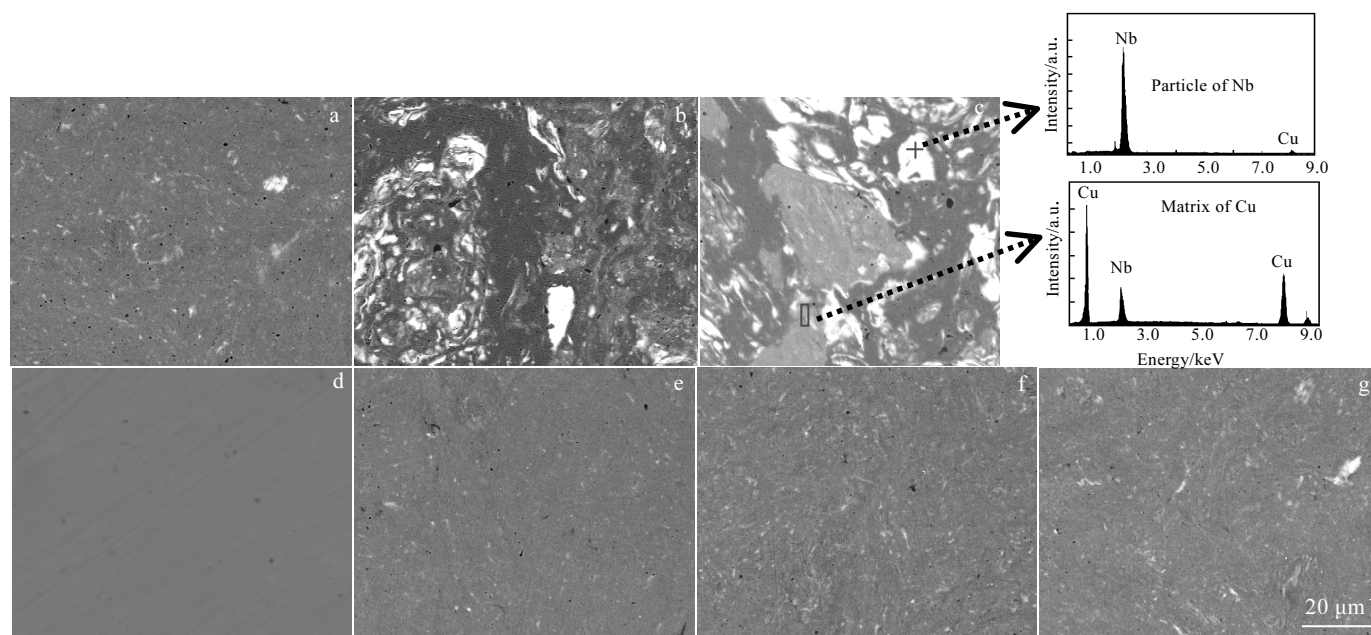
Fig.6   SEM images and EDX spectra of Cu-xNb powders milled for different time: (a) x=10 wt%, 40 h; (b) x=15 wt%, 40 h; (c) x=30 wt%, 40 h; (d) x=10 wt%, 100 h; (e) x=15 wt%, 100 h; (f) x=20 wt%, 100 h; (g) x=30 wt%, 100 h

deformed materials[22]. The discrepancy stems from the fact that the TEM image shows the actual grain size, while XRD analysis gives the size of the coherent scattering domains of crystal [22]. Fig.7b and 7c show the BF image and selected area electron diffraction pattern (SAEDP) of Cu-10wt%Nb powders milled for 100 h, respectively. It can be seen that the Cu grain size is in the order of 20 nm. Meanwhile, the SAEDP only shows the characteristic diffraction rings of Cu phase, and no diffraction spots or rings from Nb phase

can be detected, which confirms the formation of a single-phase fcc solid solution in 100 h milled Cu-10wt%Nb powders. The HRTEM image of Cu-30wt%Nb sample milled for 100 h is shown in Fig. 7d. It reveals the nanocrystalline character of the Cu matrix with the grain size below 10 nm, and also the random orientation between the crystalline grains. Furthermore, the faint Nb diffraction rings in Fig.7e reveal the incomplete solid solution of Nb into Cu in Cu-30wt%Nb powders.
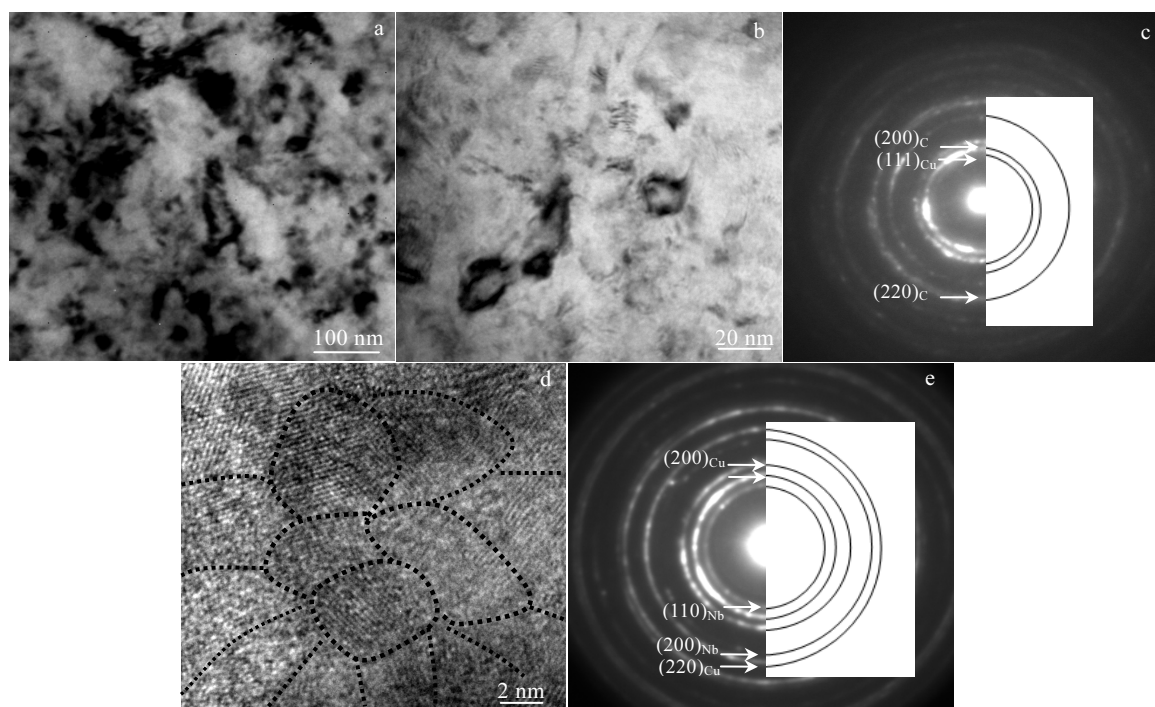
Fig.7　TEM (a, b) and HRTEM (d) images and SAEDP (c, e) of Cu-xNb powders milled for 100 h: (a) x=0 wt%, (b, c) x=10 wt%, (d, e) x=30 wt%

2.5　Microhardness measurement

Fig.8a shows the average Vickers microhardness of pure Cu and Cu-30wt%Nb samples as a function of milling time. The microhardness for both samples shows an increase with the milling time. After 100 h milling, the Cu-30wt%Nb sample reaches a microhardness value of ~4.84 GPa, which is about two times larger than that of milled pure Cu sample (~2.41 GPa). The microhardness of the Cu-Nb samples after milled for 100 h as a function of Nb concentration is plotted in Fig. 8b. The microhardness of the samples shows a noticeable increase firstly from ~2.41 GPa (pure Cu) to ~4.01 GPa (Cu-10wt%Nb), and then is enhanced with a smaller rate with higher Nb concentration.

3　Discussion

As illustrated above, the mean Cu grain size decreases with the increasing Nb concentrations for the milled Cu-Nb powders. Meanwhile, the grain size reduction has an important influence on the mechanical property of the alloys based on the Hall-Petch relation[23]. Hence, there is a strong connection among the Nb content, grain size reduction process and mechanical property of the milled Cu-Nb alloys, which is of interest to discuss in detail.

3.1　Effect of Nb content on the grain size refinement process

Generally, the grain size reduction is attributed to the mechanical energy imparted to the powders by the repeated collision between powder and balls during MA. In the present
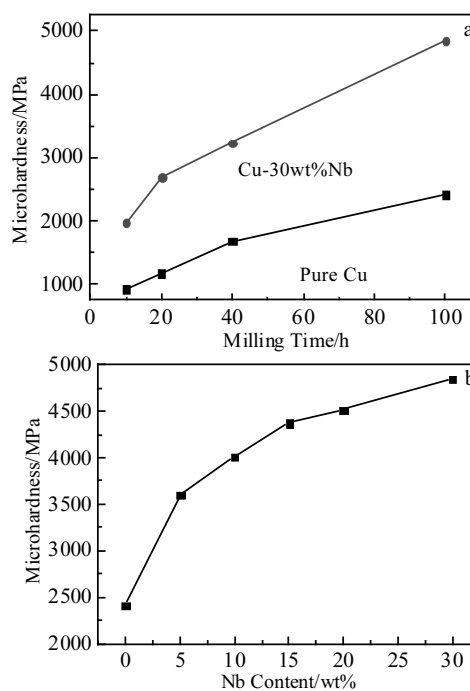

Fig.8 Microhardness for pure Cu and Cu-30wt%Nb samples versus milling time (a); microhardness of the Cu-Nb samples milled for 100 h as a function of Nb concentration (b)

case, the average Cu grain size of Cu-Nb powders is much smaller than that of the pure Cu powders milled under the same condition. For example, the mean grain size of

Cu-30wt%Nb is about four times smaller than that attained in pure Cu milled for 100 h. Therefore, it is evident that an additional grain size reduction mechanism is directly related to the Nb content.

It is well accepted that the primary factor which determines the minimum grain size of the material achieved by MA is the competition between the plastic deformation and the recovery and recrystallization processes[17]. According to the dislocation solute-pumping mechanism[24], the segregation and diffusion of Nb solutes to the dislocations of the Cu matrix take place during MA. Therefore, the dislocation motion becomes difficult owing to the solute drag effect[25], and the recovery process is inhibited, which is proved by the fact that the internal strain (dislocation density) increases with respect of Nb concentration (Fig. 4). Consequently, in the samples with higher amount of Nb solute, the susceptibility to recovery process is reduced and a higher density of structural defects can be obtained, leading to the smaller crystallite size (Fig. 9).

On the other hand, the grain size reduction process can enhance the interdiffusion between Cu-Nb elements due to the decreasing diffusion distance and increasing amount of rapid diffusion channel (non-equilibrium grain boundaries)[26]. Also, the interface energy can be improved as the grain size is reduced, and provides the additional driving force for the alloying process[27]. Once more Nb solutes are dissolved into the Cu matrix, the nanograin refinement process can be accelerated again as illustrated above. Thereby, the alloying process and the grain size reduction process induced by MA are tightly connected.

3.2 Effect of Nb content on the strengthening mechanisms

It is well known that the mechanical properties of metallic materials are determined by their inherent microstructures, especially grain sizes, solute atoms and dispersed particles. Based on the above microstructural observations, the contributions to the strengthening of the milled Cu-Nb alloys mainly include the grain boundary strengthening and the solid solution strengthening.

To find out the contribution of grain boundary strengthening from Cu nanocrystalline grains, it is better to change the microhardness values into the yield stress values. Normally, the relationship between the microhardness (H) and yield stress (σ) can be given by Tabor's relation as $H/\sigma=3$ [28]. Accordingly, the yield stress of the milled samples can be estimated on the basis of Tabor's relation. Fig.10 shows the dependence of the calculated yield stress of pure Cu and Cu-30wt%Nb samples with respect to the Cu grain size. For both samples, a linear increase in yield strength with respect to the grain size is observed, which is in agreement with the Hall-Petch relation ($\Delta\sigma_{HP}=kd^{-1/2}$)[28,29]. The calculated Hall-Petch slope values (k) for pure Cu and Cu-30wt%Nb samples are ~4795.5 MPa·nm$^{1/2}$ and ~3967 MPa·nm$^{1/2}$, respectively. The values are in the range of the
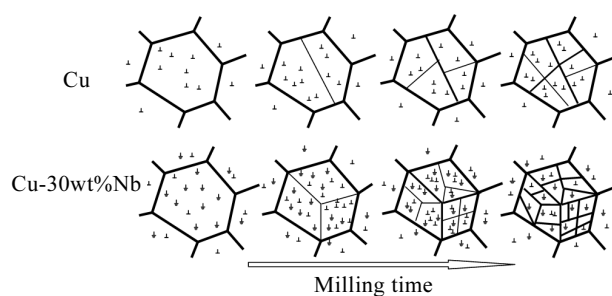

Fig.9 Schematic illustrations showing the Cu grain refinement processes of pure Cu and Cu-30wt%Nb alloy during milling
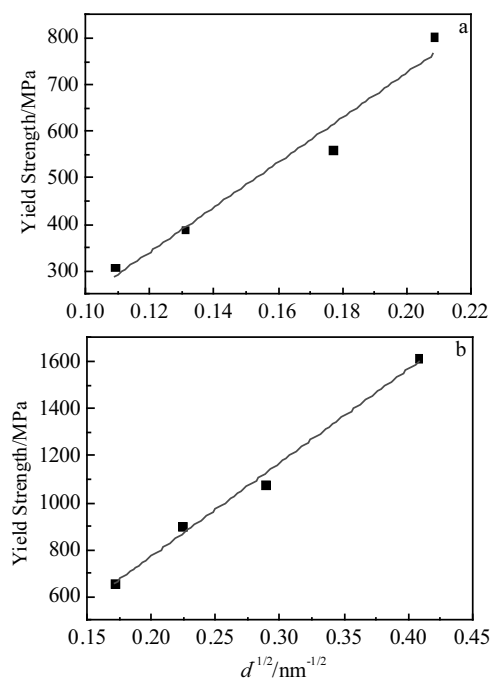

Fig.10 Hall-Petch grain size dependence of the pure Cu (a) and Cu-30wt%Nb alloy (b)

published values for nanocrystalline Cu k_{H-P}= 3500~5000 MPa·nm$^{1/2}$ [30,31]. The difference between the Hall-Petch slope values of Cu and Cu-30wt%Nb is arisen from the additional strengthening effect from the dissolved Nb solutes in Cu-30wt%Nb.

The solid solution strengthening can be approximately estimated by $\Delta\sigma_{ss}=HC^{\alpha}$, where C represents the concentration of solute atoms, α and H are positive constants[32]. Though it is hard to calculate the exact $\Delta\sigma_{ss}$ value owing to the unknown α and H values for Cu-Nb alloys, it is clear that the microhardness is enhanced as the content of dissolved Nb solute increases.

4   Conclusions

1) After 100 h of MA, a single phase Cu solid solution is formed in Cu-10wt%Nb powders. However, there are still undissolved Nb particles distributed in the Cu matrix for the

samples with higher Nb content.

2) The mean Cu grain size of the as-milled samples decreases with the increasing dissolved Nb concentration, Cu-30wt%Nb powder milled for 100 h, the average Cu grain size is only ~6 nm.

3) The microhardness of Cu-Nb samples shows an increase trend with the milling time and the amount of added Nb element. The strengthening mechanisms for nanocrystalline Cu-Nb alloys is mainly related to the grain boundary strengthening via the Hall-Petch relationship, and the solid solution strengthening from the alloying element of Nb.

References

1 Prosviryakov A S. *J Alloy Compd*[J], 2015, 632: 707

2 Dudina D V, Lomovsky O I, Valeev K R *et al. J Alloy Compd*[J], 2015, 629: 343

3 Mojtahedi M, Goodarzi M, Aboutalebi M R *et al. J Alloy Compd* [J], 2013, 550: 380

4 Bera S, Ghosh C S, Lojkowsky W *et al. Mater Sci Eng A*[J], 2012, 558: 298

5 Xi Shengqi, Zuo Kesheng, Li Xiaogang *et al. Acta Mater*[J], 2008, 56: 6050

6 Abad M D, Parker S, Kiener D *et al. J Alloy Compd*[J], 2015, 630: 117

7 Botcharova E, Freudenberger J, Schultz L. *Acta Mater*[J], 2006, 54: 3333

8 Benghalem A, Morris D G. *Mater Sci Eng A*[J], 1993, 161: 255

9 Abad M D, Parker S, Kiener D *et al. J Alloy Compd*[J], 2015, 630: 117

10 Mula S, Bahmanpour H, Mal S *et al. Mater Sci Eng A*[J], 2012, 539: 330

11 Botcharova E, Heilmaier M, Freudenbergera J *et al. J Alloy Compd*[J], 2003, 351: 119

12 Lei R S, Wang M P, Li Z *et al.*   *Mater Sci Eng A*[J], 2011, 528: 4475

13 Kapoor M, Kaub T, Darling K A *et al. Acta Materialia*[J], 2017, 126: 564

14 Wang T L, Li J H, Tai K P *et al. Scripta Mater*[J], 2007, 57: 157

15 Lei R S, Wang M P, Wang H P *et al. Mater Charact*[J], 2016, 118: 324

16 Lei R S, Wang M P, Li Z *et al. Mater Sci Eng A*[J], 2011, 528: 4475

17 Suryanarayana C. *Prog Mater Sci*[J], 2001, 46: 1

18 Contini A, Delogu F, Garroni S *et al. J Alloy Compd*[J], 2014, 615: S551

19 Michaelsen C, Gente C. *J Appl Phys*[J], 1997, 81: 6024

20 Pearson W B. *A Handbook of Lattice Spacings and Structures of Metals and Alloys*[M], Oxford: Pergamon, 1967

21 Raabe D, Ohsaki S, Hono K. *Acta Mater*[J], 2009, 57: 5254

22 Kursun C, Gogebakan M. *J Alloy Compd*[J], 2015, 619: 138

23 Hu J, Shi Y N, Sauvage X *et al. Science*[J], 2017, 355(2): 1292

24 Michels A, Krill C E, Ehrhardt H *et al. Acta Mater*[J], 1999, 47: 2143

25 Muthaiah V M S, Mula S. *J Alloy Compd*[J], 2016, 688: 571

26 Huang J Y, Yu Y D, Wu Y K *et al. Acta Mater*[J], 1997, 45: 113

27 Zhao Y H, Lu K. *Phys Rev B*[J], 2002, 66: 085 404

28 Rajulapati K V. *Materials Science and Engineering*[D], North Carolina: North Carolina State University, 2007

29 Chen Y, Gao N, Sha G *et al. Acta Materialia*[J], 2016, 109: 202

30 Armstrong R W. *Proceedings of 5th International Conference on the Strength of Metals and Alloys*[C]. Aachen, Germany: ICSMA, 1979: 27

31 Zhao M, Li J C, Jiang Q. *J Alloy Compd*[J], 2003, 361: 160

32 Darling K A, Roberts A J, Armstrong L. *Mater Sci Eng A*[J], 2014, 589: 57

Nb 含量对机械合金化 Cu-Nb 合金晶粒细化和力学性能的影响

雷若姗 [1]，陈广润 [1]，汪明朴 [2]
(1. 中国计量大学，浙江 杭州 310018)
(2. 中南大学， 湖南 长沙 410083)

摘　要: 采用机械合金化法制备了质量分数 x=0%~30% 的 Cu-xNb 合金粉末，通过 X 射线衍射仪(XRD)、金相显微镜(OM)、扫描电镜(SEM)、透射电镜(TEM)观察和显微硬度测量分析了 Nb 溶质含量对粉末晶粒细化过程以及力学性能的影响。结果表明，尽管 Nb 与 Cu 的平衡固溶度接近为 0，经 100 h 球磨后，Nb 在 Cu 中的最大固溶量可达约 11%。随着 Nb 含量的增加，Cu-Nb 合金粉末的晶粒细化能力提高。这是由于随着偏析至位错处的溶质原子数量增加，合金的回复过程得到抑制，因此有利于晶粒尺寸的减小。Cu-30%Nb 合金球磨 100 h 后 Cu 相平均晶粒尺寸减小至约 6 nm。此外，球磨 Cu-Nb 合金粉末的显微硬度随着 Nb 含量的增加而提高，其强化机制主要为细晶强化和固溶强化。

关键词: 铜合金；　纳米晶；机械合金化；过饱和固溶体；显微硬度